



Dalton
Transactions

Synthesis, structure and DFT calculation of a mononuclear cyclic (alkyl)(amino) carbene supported Titanium(II) complex

Journal:	<i>Dalton Transactions</i>
Manuscript ID	DT-COM-08-2019-003342.R1
Article Type:	Communication
Date Submitted by the Author:	16-Sep-2019
Complete List of Authors:	Ma, Wangyang; Southern University of Science and Technology, Department of Chemistry Zhang, Jing-Xuan; The Hong Kong University of Science and Technology, Department of Chemistry Lin, Zhenyang; The Hong Kong University of Science and Technology, Department of Chemistry Tilley, T. Don; University of California, Berkeley, Chemistry Ye, Qing; Southern University of Science and Technology, Department of Chemistry

SCHOLARONE™
Manuscripts

Synthesis, Structure and DFT Calculations of Mononuclear Cyclic (Alkyl)(amino) Carbene supported Titanium(II) Complexes

 Wangyang Ma,^a Jing-Xuan Zhang,^b Zhenyang Lin,^{*b} T. Don Tilley,^c and Qing Ye^{*a,d}

 Received 00th January 20xx,
 Accepted 00th January 20xx

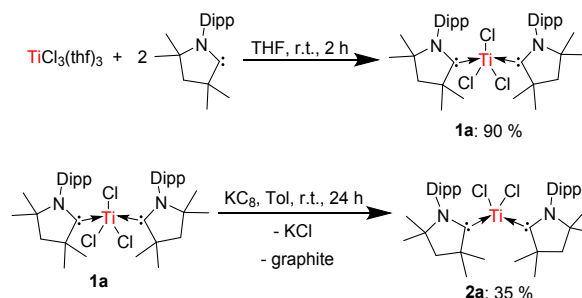
DOI: 10.1039/x0xx00000x

www.rsc.org/

The mononuclear cyclic (alkyl)(amino)carbene (cAAC) supported titanium(III) chloride complex [(cAAC)₂TiCl₃] has been synthesized by treatment of free cAAC with TiCl₃(THF)₃. Further reduction of (cAAC)₂TiCl₃ with potassium graphite (KC₈) afforded the desired (cAAC)₂TiCl₂ complex, which features a small S-T energy gap. Both complexes were structurally characterized and represent the first cAAC supported Ti complexes.

Titanium complexes are widely used as catalysts in organic synthesis such as McMurry coupling and Kulinkovich cyclopropanation reactions.^[1] While the chemistry of titanium is dominated by the +4 and +3 oxidation states, the low-valent titanium species are of significance to mechanistic studies, since they are often considered as key intermediates in catalytic cycles.^[2] The general synthetic approach to low-valent Ti species is chemical reduction of their high valent titanium precursors.^[3] Nevertheless, isolable low-valent complexes are rare, and well-defined Ti^{II} (3d²) complexes remain scarce and less studied. Only a handful of reports on L_nTiCl₂ complexes were reported and L are limited to amine and pyridine ligands.^[4] In recent years, various cyclic (alkyl)(amino)carbenes (cAACs) have been successfully synthesized. Thanks to their strong σ-donating and π-accepting character, they have been widely applied as supporting ligands for stabilizing highly reactive main group species as well as low-valent late transition metal (TM = Au, Cu, Co, Fe, Ni, Mn and Zn) complexes.^[5] Notably, this strategy has been far less utilized to stabilize low-valent early transition metal centers. There are numerous group 4 transition

metal complexes (in various oxidation states) that contain NHC ligands.^[6] Very recently, Deng and co-workers have synthesized and structurally characterized the low-valent and low-coordinate (cAAC)₂Hf^{II}X₂ (X = Cl, CH₂Ph) species as the first examples of group IV transition metal complexes supported by cAAC ligands. Furthermore, the Hf(II) cAAC complexes have turned out to be diamagnetic with closed-shell ground states.^[7] Given the fact that the first transition-series elements of a given group show considerably different chemical properties from their heavy congeners and based on our previous work,^[8] we were motivated to synthesize and investigate Ti(II) examples. Herein, we report the synthesis and characterization of a four-coordinate titanium(II) bis(cAAC) complex, which represents the first example of a cAAC stabilized, formally Ti(II) species.



Scheme. 1 Synthesis of **1a** and **2a**.

The (cAAC)₂Ti(III)Cl₃ complex **1a** was prepared as a purple crystalline solid in high isolated yield (90%) from the reaction of readily available TiCl₃(THF)₃^[9] with 2 equivalents of cAAC ligand in THF (Scheme. 1). An immediate color change from blue to purple was observed and large crops of purple crystals were obtained upon slow evaporation of a Et₂O solution of the crude product at -30 °C. Notably, complex **1a** is sensitive to air and moisture. Due to its paramagnetism, ¹H NMR spectrum showed broad peaks that cannot be assigned. Complex **1a** has been characterized by EPR spectroscopy, elemental analysis, and X-ray single-crystal structural analysis. The EPR spectrum (Fig. S1

^a Department of Chemistry, Southern University of Science and Technology, Shenzhen, Guangdong 518055, China. E-mail: yeq3@sustech.edu.cn

^b Department of Chemistry, The Hong Kong University of Science and Technology, Clear Water Bay, Kowloon, Hong Kong, China

^c Department of Chemistry, University of California, Berkeley, Berkeley, California 94720-1460, United States

^d School of Chemistry and Chemical Engineering, Southeast University, Nanjing 210089, China.

† Electronic supplementary information (ESI) available. CCDC 1910420 and 1910434. For ESI and crystallographic data in CIF or other electronic format see DOI: XXX

in SI) of a toluene solution of **1a** at room temperature display an isotropic signal centered at a g value of 1.97, suggesting that the unpaired electron is primarily metal-centered, but more distributed on the cAAC ligands than in $(\text{IPr})_2\text{TiCl}_3$ ($g = 1.91$; $\text{IPr} = 1,3\text{-bis}(2,6\text{-diisopropylphenyl})\text{imidazol-2-ylidene}$).^[10]

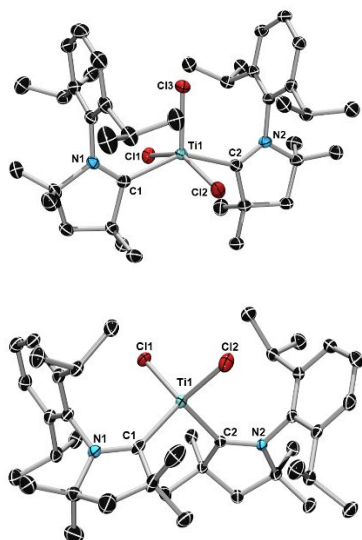


Fig. 1 Molecular structures of complex **1a** (top) and **2a** (bottom) in the solid state (ellipsoids set at 50% probability). Hydrogen atoms are omitted for clarity. Selected bond distances (Å) and angles (°) for **1a**: Ti1–C1 2.298(2), Ti1–C2 2.301(2), Ti1–Cl1 2.3611(6), Ti1–Cl2 2.3488(6), Ti1–Cl3 2.2342(6), C1–N1 1.318(3), C2–N2 1.316(3); C1–Ti1–C2 147.35(7), C1–Ti1–Cl2 149.47(3); for **2a**: Ti1–C1 2.095(3), Ti1–C2 2.122(2), Ti1–Cl1 2.2647(8), Ti1–Cl2 2.2854(8), C1–N1 1.372(3), C2–N2 1.353(3); C1–Ti1–C2 105.60(9), C1–Ti1–Cl2 116.75(3).

The molecular structure of **1a** is shown in Fig. 1 (top). The geometry around the titanium center can be regarded as a strongly distorted trigonal bipyramid with the two cAAC ligands in the axial positions and three chlorides in equatorial positions. However, in sharp contrast to the Ti^{III} bis(NHC) complex $(\text{IPr})_2\text{TiCl}_3$ that features a nearly linear axis ($176.3(2)^\circ$),^[10] the axial angle of $147.35(7)^\circ$ in **1a** greatly deviates from the ideal 180° . Correspondingly, two equatorial Cl atoms (Cl1, Cl2) scissor out ($120^\circ \rightarrow 147.35(7)^\circ$), forming together with C1 and C2 atoms a square, and thus leading to an overall geometry of a square-based pyramid with Cl3 atom as the pivot ligand. DFT calculation suggested that the distortion is determined by electronic factor (Table S5 and Fig. S10). The Ti–C(cAAC) bond lengths (2.298(2) Å, 2.301(2) Å) are somewhat shorter than those in the $(\text{IPr})_2\text{Ti}^{\text{III}}\text{Cl}_3$ complex [2.336(4) Å (av.)],^[10] which is attributed to the stronger σ -donating and π -accepting character of cAACs versus NHCs, but are remarkably longer than the Ti–C σ -bonds in previously reported titanium alkyl complexes (210–220 pm).^[8] The N–C(cAAC) bond lengths (1.318(3) Å, 1.316(3) Å) are within the range of those for the free cAAC ligand (1.315(3) Å).^[11]

Reduction of $(\text{cAAC})_2\text{TiCl}_3$ (**1a**) with an equimolar amount of potassium graphite (KC_8) in toluene at room temperature afforded the desired product $(\text{cAAC})_2\text{TiCl}_2$ (**2a**) as dark black

crystalline solids in acceptable yield (35%). Complex **2a** was fully characterized by multinuclear NMR spectroscopy, elemental analysis, and single-crystal X-ray diffraction analysis (Fig. 1, bottom). The low-valent Ti complex **2a** is extremely air and moisture sensitive, but stable as a solid under nitrogen atmosphere for 2 weeks without noticeable decomposition.

The single crystal structure of complex **2a** displayed a distorted tetrahedral geometry around the Ti center. The Ti–C(cAAC) bond lengths (2.095(3) Å, 2.122(2) Å) are significantly shorter in comparison to those in the $(\text{cAAC})_2\text{TiCl}_3$ precursor. Furthermore, the N–C(cAAC) bond lengths (1.372(3) Å, 1.353(3) Å) are elongated with respect to that of the free cAAC ligand (1.315(3) Å).^[11] These structural features indicate delocalization of the two d electrons derived from the Ti center within the N1–C1–Ti1–C2–N2 skeleton *via* π interactions. Furthermore, the C(cAAC)–Ti–C(cAAC) angle of $105.60(9)^\circ$ is more acute than that in the $(\text{cAAC})_2\text{HfCl}_2$ congener ($113.81(4)^\circ$).^[7]

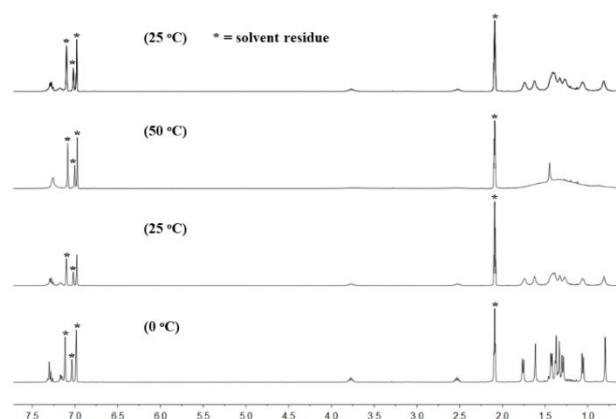


Fig. 2 Reversible temperature dependent change on ^1H NMR spectra of **2a** from 0°C via 25°C to 50°C and back to 25°C .

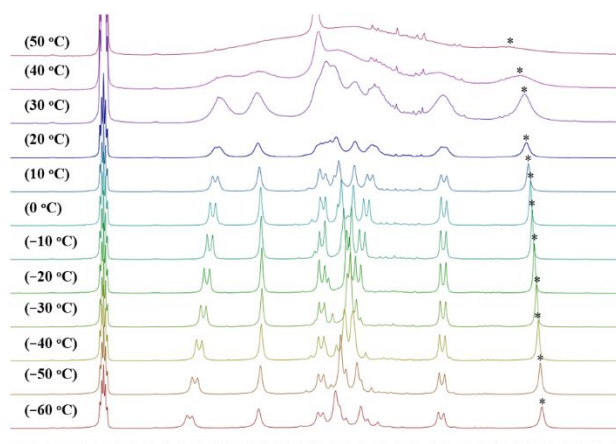


Fig. 3 Variable temperature 400 MHz ^1H NMR spectra of **2a** in $\text{tol-}d_8$ from -60°C to 50°C with noticeable chemical shifts change at ~ 0.78 ppm (marked with *).

In contrast to the recently reported Hf(II) bis(cAAC) complex, the ^1H NMR spectrum of complex **2a** at ambient temperature (25°C) showed broad signals that are poorly resolved. The

broadening of resonances suggests partial thermal population of a triplet state that is slightly higher in energy than the diamagnetic singlet ground state. This assumption was confirmed by variable temperature 400 MHz ^1H NMR spectra, which showed strongly temperature dependent and fully reversible spectroscopic behavior. The spectra displayed very broad and unresolved signals at higher temperatures, and sharpening of resonances upon cooling the sample. The ^1H NMR spectrum at 0 $^\circ\text{C}$ is nearly identical with the diamagnetic $(\text{cAAC})_2\text{HfCl}_2$ ^[7] and remains unchanged at lower temperatures (Fig. 2). Furthermore, the singlet–triplet equilibrium that gives rise to the paramagnetism was quantified from VT- ^1H NMR of **2a** according to the literature,^[12] which allows a determination of the singlet–triplet energy gap ($\Delta E_{\text{T-S}}$). Noting that the singlet signal at 0.78 ppm clearly shifts over the range of -60 $^\circ\text{C}$ to 50 $^\circ\text{C}$, fitting of the chemical shift vs temperature data gave a small energy difference between the two states for $\text{CAAC}_2\text{TiCl}_2$ of 0.52 kcal/mol (Fig. 3, see SI for more fitting details).

To gain in-depth insight into the electronic structure of complex **2a**, DFT calculations were performed by optimizing the structure of compound **2a** in both singlet and triplet states and comparing their relative stabilities. A singlet biradical state has been located as the electronic ground state, slightly below a low-lying triplet state by 0.47 kcal/mol. This result is in good agreement with the experimentally determined value (0.52 kcal/mol). In addition, the singlet biradical state also has a shorter Ti–C(cAAC) distance that better agrees with the crystal structure.

To investigate the spin crossover behavior of complex **2a**, we further calculated the relative free energies between the singlet biradical state and triplet state of complex **2a** at various temperatures (Table S4 and Fig. S9). The results show that at zero Kelvin, the Gibbs free energy of the singlet biradical state is still 0.30 kcal/mol lower than that of the triplet state, consistent with the experimental fact that the Ti(II) complex is found to be diamagnetic at low temperature. On the other hand, the Gibbs free energy gap of the triplet state relative to the singlet biradical state keeps decreasing when the temperature is raised, in agreement with the experimentally observed spin crossover. According to the calculation results, the theoretically predicted spin crossover occurs at around 70 K. Clearly, this theoretically predicted spin crossover temperature is far below the experimentally observed value (Fig. 3). As we will see later, the stability of the triplet state at high temperature is purely a result of entropic stabilization. We know that computationally a very accurate evaluation of the entropic contribution is not possible. However, our computational results qualitatively agree with the experimental finding that the triplet state is favored at high temperature.

To achieve a deeper understanding of the observed spin crossover, a Spin Natural Orbital (SNO) analysis has been performed on the two calculated electronic states of the Ti(II) complex. In the singlet biradical state, SNO analysis shows that the unpaired electrons are localized on the two cAAC carbon atoms, one with excess alpha spin density and the other one with excess beta spin density, both partially delocalized to the Ti center, as shown in Fig. 4(a). In the triplet state, the two

unpaired electrons are both localized on the Ti atom as shown in Fig. 4(b). It can be clearly seen that the Ti center has utilized two Ti 3d orbitals for Ti–C(cAAC) π -bonding in the singlet biradical state, each bonded with one NHC ligand, while only one 3d orbital is involved in a delocalized C(cAAC)–Ti–C(cAAC) π -bonding in the triplet state. This will lead to a stronger Ti–C(cAAC) bond as well as a larger force constant for the Ti–C(cAAC) bond vibration in the singlet biradical state than in the triplet state, as indicated by the different Ti–C(cAAC) bond distances (Fig. 5), which may explain why the singlet biradical state is electronically favored but entropically disfavored compared to the triplet state. In addition, a smaller C(cAAC)–Ti–C(cAAC) bond angle is found for the singlet biradical state (Fig. 5), which may lead to more constrained molecular bending and may also contribute to the higher free energy of the singlet biradical state at higher temperature.

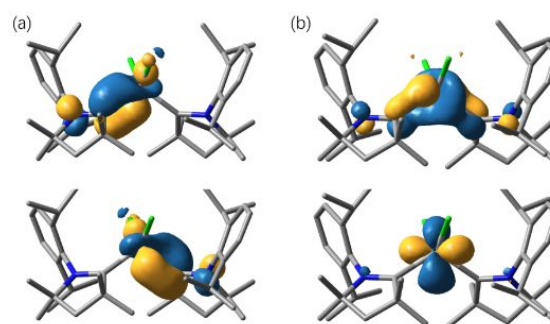


Fig. 4. Spin Natural Orbitals (SNO) calculated for the Ti(II) complex at (a) singlet biradical state, and (b) triplet state.

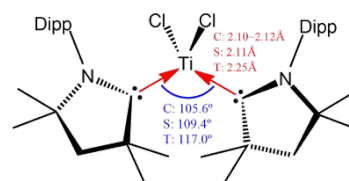


Fig. 5. Lewis structure of the complex **2a** with selected structural parameters labeled. C, S, and T stand for experimental crystal structure, calculated singlet biradical, and calculated triplet, respectively.

In summary, we have synthesized and characterized the first mononuclear cyclic (alkyl)(amino) carbene-supported titanium(II) complex. Variable temperature ^1H NMR spectra reveal a small energy gap of 0.52 kcal/mol between the singlet ground state and the triplet state, which was further confirmed by DFT calculations. According to the computational results, the singlet biradical state is the ground state and is electronically favored, but entropically disfavored when compared to the triplet state. Further reaction chemistry of cAAC-supported low-valent titanium complexes is in progress in our laboratory.

This work was supported by the Science and Technology Innovation Commission of Shenzhen Municipality (JCYJ20170817104802070), start-up fund from SUSTech and the Research Grants Council of Hong Kong (HKUST16304017). TDT

would like to thank the National Science Foundation for support, under grant CHE-1566538. The authors also thank Dr. Ivo Krummenacher (University of Würzburg) for helpful discussions on EPR spectra analysis.

Conflicts of interest

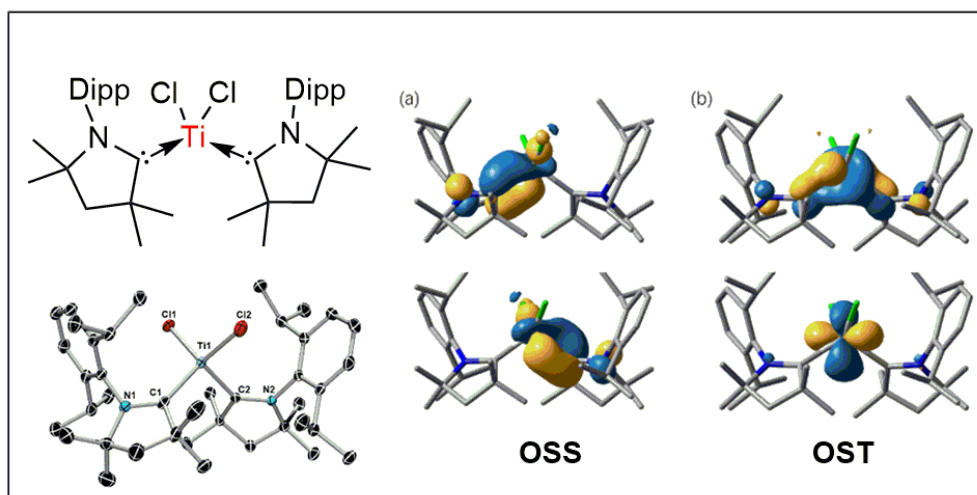
The authors declare no conflict of interest.

Notes and references

- 1 (a) J. E. McMurry, *Chem. Rev.*, 1989, **89**, 1513–1524; (b) O. G. Kulinkovich, S. V. Sviridov and D. A. Vasilevski, *Synthesis*, 1991, 234–234.
- 2 (a) R. H. Crabtree, *Organometallic Chemistry of the Transition Metals*, John Wiley & Sons, Hoboken, New Jersey, 2014; (b) E. P. Beaumier, A. J. Pearce, X. Y. See and I. A. Tonks, *Nat. Rev. Chem.*, 2019, **3**, 15–34.
- 3 U. Rosenthal, V. V. Burlakov, P. Arndt, W. Baumann and A. Spannenberg, *Organometallics*, 2003, **22**, 884–900.
- 4 (a) J. J. H. Edema, R. Duchateau, S. Gambarotta, R. Hynes and E. Gabe, *Inorg. Chem.*, 1991, **30**, 154–156; (b) G. B. Wijeratne, E. M. Zolnhofer, S. Fortier, L. N. Grant, P. J. Carroll, C.-H. Chen, K. Meyer, J. Krzystek, A. Ozarowski, T. A. Jackson, D. J. Mindiola and J. Telsler, *Inorg. Chem.*, 2015, **54**, 10380–10397; (c) M. A. Araya, F. A. Cotton, J. H. Matonic and C. A. Murillo, *Inorg. Chem.*, 1995, **34**, 5424–5428.
- 5 (a) M. Melaimi, R. Jazzar, M. Soleilhavoup and G. Bertrand, *Angew. Chem., Int. Ed.*, 2017, **56**, 10046–10068; (b) M. Soleilhavoup and G. Bertrand, *Acc. Chem. Res.* 2015, **48**, 256–266; (c) C. D. Martin, M. Soleilhavoup and G. Bertrand, *Chem. Sci.* 2013, **4**, 3020–3030; (d) M. Melaimi, M. Soleilhavoup and G. Bertrand, *Angew. Chem., Int. Ed.*, 2010, **49**, 8810–8849; (e) S. Roy, K. C. Mondal and H. W. Roesky, *Acc. Chem. Res.*, 2016, **49**, 357–369; (f) U. S. D. Paul and U. Radius, *Eur. J. Inorg. Chem.*, 2017, 3362–3375. (g) A. A. Danopoulos, T. Simler and P. Braunstein, *Chem. Rev.* 2019, **119**, 3730–3961.
- 6 D. Zhang and G. Zi, *Chem. Soc. Rev.* 2015, **44**, 1898–1921.
- 7 Q. Liu, Q. Chen, X. Leng, Q.-H. Deng and L. Deng, *Organometallics*, 2018, **37**, 4186–4188.
- 8 Q. Ye, M. S. Ziegler, K. V. and T. Don. Tilley, *Eur. J. Inorg. Chem.*, 2017, 2484–2487.
- 9 N. A. Jones, S. T. Liddle, C. Wilson and P. L. Arnold, *Organometallics*, 2007, **26**, 755–757.
- 10 J. Li, C. Schulzke, S. Merkel, H. W. Roesky, P. P. Samuel, A. Döring and D. Stalke, *Z. Anorg. Allg. Chem.*, 2010, **636**, 511–514.
- 11 V. Lavallo, Y. Canac, C. Präsang, B. Donnadiu and G. Bertrand, *Angew. Chem., Int. Ed.*, 2005, **44**, 5705–5709.
- 12 (a) C. M. Lemon, M. Huynh, A. G. Maher, B. L. Anderson, E. D. Bloch, D. C. Powers and D. G. Nocera, *Angew. Chem. Int. Ed.*, 2016, **55**, 2176–2180; (b) B. Le Guennic, T. Floyd, B. R. Galan, J. Autschbach and J. B. Keister, *Inorg. Chem.* 2009, **48**, 5504–5511.

RSC Author Templates - ChemDraw (CDX) - Graphical Abstracts

All text and images must be placed within the frame.



81x71mm (300 x 300 DPI)